Climate Dynamics (2006) 26: 513–529
DOI 10.1007/s00382-005-0081-9

**V. Masson-Delmotte · M. Kageyama · P. Braconnot
S. Charbit · G. Krinner · C. Ritz · E. Guilyardi
J. Jouzel · A. Abe-Ouchi · M. Crucifix
R. M. Gladstone · C. D. Hewitt · A. Kitoh
A. N. LeGrande · O. Marti · U. Merkel · T. Motoi
R. Ohgaito · B. Otto-Bliesner · W. R. Peltier
I. Ross · P. J. Valdes · G. Vettoretti · S. L. Weber
F. Wolk · Y. YU**

Past and future polar amplification of climate change: climate model intercomparisons and ice-core constraints

Received: 31 May 2005 / Accepted: 22 September 2005 / Published online: 20 December 2005

Abstract Climate model simulations available from the PMIP1, PMIP2 and CMIP (IPCC-AR4) intercomparison projects for past and future climate change simulations are examined in terms of polar temperature changes in comparison to global temperature changes and with respect to pre-industrial reference simulations. For the mid-Holocene (MH, 6,000 years ago), the models are forced by changes in the Earth's orbital parameters. The MH PMIP1 atmosphere-only simulations conducted with sea surface temperatures fixed to modern conditions show no MH consistent response for the poles, whereas the new PMIP2 coupled atmosphere–ocean climate models systematically simulate a significant MH warming both for Greenland (but smaller than ice-core based estimates) and Antarctica (consistent with the range of ice-core based range). In both PMIP1 and

V. Masson-Delmotte (✉) · M. Kageyama · P. Braconnot
S. Charbit · E. Guilyardi · J. Jouzel · O. Marti
Laboratoire des Sciences du Climat et de l'Environnement,
(LSCE/IPSL, UMR CEA-CNRS 1572) L'Orme des Merisiers,
Bâtiment 701, CEA Saclay, 91 191 Gif-sur-Yvette Cedex, France
E-mail: valerie.masson@cea.fr

G. Krinner · C. Ritz
Laboratoire de Glaciologie et de Géophysique de l'Environnement,
(UMR 5183 CNRS-UJF), Domaine Universitaire, St Martin
d'Hères, France

A. Abe-Ouchi
Center for Climate System Research, The University of Tokyo,
Kashiwa, 277-8568 Japan

M. Crucifix · C. D. Hewitt
Hadley Centre for Climate Prediction and Research, Met Office,
FitzRoy Road, Exeter, EX1 3 PB Devon, UK

R. M. Gladstone · I. Ross · P. J. Valdes
School of Geographical Sciences,
University of Bristol,
University Road, Bristol, BS8 1SS UK

A. Kitoh · T. Motoi
Climate Research Department,
Meteorological Research Institute,
1-1 Nagamine, Tsukuba,
Ibaraki, 305-0052 Japan

A. N. LeGrande
NASA Goddard Institute for Space Studies and
Center for Climate Systems Research, Columbia University,
New York, NY, USA

U. Merkel
IFM-GEOMAR,
Duesternbrooker Weg 20,
24105 Kiel, Germany

R. Ohgaito · A. Abe-Ouchi
Frontier Research Center for Global Change (FRCGC),
JAMSTEC, Yokohama City, 236-0001 Japan

B. Otto-Bilesner
Climate Change Research,
National Center for Atmospheric Research,
1850 Table Mesa Drive, P.O. Box 3000,
Boulder, CO, 80307 USA

W. R. Peltier · G. Vettoretti
Department of Physics, University of Toronto,
60 St. George Street, Toronto,
ON, M5S 1A7 Canada

S. L. Weber
Climate Variability Research,
Royal Netherlands Meteorological Institute (KNMI),
P.O. Box 201, 3730 AE De Bilt, The Netherlands

F. Wolk
Institut d'Astronomie et de Géophysique G. Lemaître,
Université catholique de Louvain, Chemin du cyclotron, 2,
1348 Louvain-la-Neuve, Belgium

Y. Yu
LASG, Institute of Atmospheric Physics,
Chinese Academy of Sciences,
P.O. Box 9804, Beijing, 10029
People's Republic of China

PMIP2, the MH annual mean changes in global temperature are negligible, consistent with the MH orbital forcing. The simulated last glacial maximum (LGM, 21,000 years ago) to pre-industrial change in global mean temperature ranges between 3 and 7°C in PMIP1 and PMIP2 model runs, similar to the range of temperature change expected from a quadrupling of atmospheric CO_2 concentrations in the CMIP simulations. Both LGM and future climate simulations are associated with a polar amplification of climate change. The range of glacial polar amplification in Greenland is strongly dependent on the ice sheet elevation changes prescribed to the climate models. All PMIP2 simulations systematically underestimate the reconstructed glacial–interglacial Greenland temperature change, while some of the simulations do capture the reconstructed glacial–interglacial Antarctic temperature change. Uncertainties in the prescribed central ice cap elevation cannot account for the temperature change underestimation by climate models. The variety of climate model sensitivities enables the exploration of the relative changes in polar temperature with respect to changes in global temperatures. Simulated changes of polar temperatures are strongly related to changes in simulated global temperatures for both future and LGM climates, confirming that ice-core-based reconstructions provide quantitative insights on global climate changes.

1 Introduction

The Arctic (Corell et al. 2004) and the Antarctic Peninsula (Jacka and Budd 1998; Vaughan et al. 2003) are experiencing some of the most rapid temperature rises on Earth. Since the 1960s, temperatures have risen by more than 2°C in some areas, several times more rapidly than the average global temperature (IPCC 2001; Moritz et al. 2002). Due to possible changes in snow and ice cover and associated albedo feedbacks, polar regions are likely to act as amplifiers of climate change, however modulated by local processes generating multi-decadal variability (Bengtsson et al. 2004; Polyakov et al. 2002). Future climate change simulations in the Arctic indeed show a polar amplification with 1.5–4.5 times the global warming (Holland and Bitz 2003). These contrasted results apparently result from three main processes in the climate models: different changes in cloud cover (and cloud radiative feedbacks); different changes in heat advection (Alexeev et al. 2005); and, most important, different response in sea–ice. The level of future polar amplification was indeed shown to be dependent on the modern sea–ice thickness and snow cover simulations (Dixon et al. 2003; Holland and Bitz 2003). Early studies have revealed that models with cold modern biases, when forced with increased greenhouse gas concentrations, had a larger sensitivity due to a larger ice feedback (Dixon et al. 2003; Rind et al. 1997). Reducing the uncertainties of future climate change predictions is extremely important for high latitude areas because (1) local eco-systems will be extremely vulnerable to large warmings because of competition with living organisms from lower latitudes more adapted to warm conditions, and impossibility of migration to colder places (Corell and coauthors 2004); (2) ice sheets are susceptible to respond to a fast warming (Rignot and Thomas 2002), either by increased accumulation (Huybrechts et al. 2004) or coastal thinning (Krabill et al. 2004) and modify the freshwater supply to the high latitude oceans; (3) the warming of the Arctic may increase the release of carbon from soils and act as a positive feedback on climate change (Knorr et al. 2005).

In order to assess the capacity of state-of-the-art climate models to simulate realistically the high latitude climate changes, past climate simulations are compared here with ice-core estimates for last glacial maximum (21,000 years ago, hereafter LGM) and mid-Holocene (6,000 years ago, hereafter MH) temperature changes. These simulations enable the test of the model responses to a variety of forcings. MH boundary conditions include pre-industrial greenhouse gas levels together with modified orbital parameters (Berger 1978) which induce small changes in low to high latitude annual mean insolation (effect of obliquity change), but with a seasonal cycle increased (respectively reduced by locally ~5%) in the northern (respectively southern) hemisphere (in response to precession changes). In this respect, polar MH simulations provide a test of climate model response mainly to a modified seasonal cycle forcing (Renssen et al. 2005a, b). LGM boundary conditions include reduced atmospheric greenhouse gas levels (CO_2, CH_4 and N_2O), modified surface boundary conditions including the presence of massive ice sheets over northern North America and Fennoscandia (Peltier 1994, 2004) and small changes in orbital parameters (Table 1).

Climate models offer unique frames to understand the spatial representativity of polar ice core sites. In particular, glacial–interglacial Antarctic temperature changes have been used to estimate paleoclimatic constraints on climate sensitivity, assuming that they are representative of global temperature changes (Genthon et al. 1987; Lorius et al. 1990; Manabe and Broccoli 1985). In this paper, we review the global and polar temperature response of new past and future climate simulations conducted with state-of-the-art coupled climate models with standardized forcings. We have used the database of Coupled Models Intercomparison Project (CMIP, http://www.pcmid.llnl.gov/ipcc, database as of 15.04.2005) and second phase of the Paleoclimate Modelling Intercomparison Project (PMIP2, http://www.lsce.cea.fr/pmip2 database of 15.09.2005) (Harrison et al. 2002). These recent model intercomparison results are currently used as part of the fourth IPCC assessment. They are also compared to earlier simulations conducted with atmosphere alone models (Paleoclimate Modelling Intercomparison Project, PMIP, http://www.lsce.cea.fr/pmip, Joussaume and Taylor 1995).

Table 1 Boundary conditions used for the past and future climate simulations

Simulations	Atmospheric composition (greenhouse gases)	Land surface	Ocean surface	Orbital parameters	Years analysed
$2\times CO_2$	1 ppm/year increase until CO_2 doubling (70 years) then stabilization	Modern	Calculated	Modern	Years 120–170
Control run	Pre-industrial ~280 ppm CO_2				First 50 years of the simulations
$4\times CO_2$	1 ppm/year increase until CO_2 quadrupling (140 years) then stabilization	Modern	Calculated	Modern	Years 190–240
Control run	Pre-industrial ~280 ppm CO_2				First 50 years of the simulations
PMIP1 MH fixed SST "fix"	Pre-industrial	Modern	Fixed to modern	6,000 BP	All years in database (equilibrium simulations)
Control run	Modern			Modern	
PMIP2 MHCoupled models "cpl"	Pre-industrial	Modern or interactively calculated (OAV models)	Calculated	6,000 BP	All years in database (equilibrium simulations)
Control run				Modern	
PMIP1 LGM fixed SST "fix"	Glacial 200 ppmv	Vegetation : modern, Ice sheets, coastline : (Peltier 1994)	Fixed to (CLIMAP 1981)	21,000 BP	All years in database (equilibrium simulations)
Control run	Modern	Modern	Modern	Modern	
PMIP1 LGM Computed SST "slab"	Glacial 200 ppmv	Vegetation: modern, Ice sheets, coastline : (Peltier 1994)	Slab ocean	21,000 BP	All years in database (equilibrium simulations)
Control run	Modern	Modern		Modern	
Post-PMIP1 LGM Coupled models "cpl"	Glacial 185 ppmv	Vegetation: control, Ice sheets, (Peltier 1994, 2004) Coastline : either unchanged or −105 m	Calculated	21,000 BP	All years in database (equilibrium simulations)
Control run	Modern except HadCM3 (Pre-industrial)	Modern		Modern	
PMIP2 LGM Coupled models "cpl"	Glacial 185 ppmv	Vegetation: control, Coastline : −105 m, Ice sheets, (Peltier 2004)	Calculated	21,000 BP	All years in database (equilibrium simulations)
Control run	Pre-industrial	Modern		Modern	

For the description of the different models please refer to the CMIP and PMIP database description (http://www.lsce.cea.fr/pmip/, http://www.lsce.cea.fr/pmip2/, http://www.pcmdi.llnl.gov/ipcc/about_ipcc.php)

The key questions we address are: what is the performance of the models in simulating past climate changes at the poles? Is there a polar amplification under different forcings? How do relationships between global and polar temperature changes vary for radically different climates such as the LGM and increased CO_2 experiments?

2 LGM and MH climate change: polar ice core data

Deep polar ice cores offer unique archives of past climate and environmental changes extending over several climatic cycles in East Antarctica, at Vostok (Petit et al. 1999), Dome F (Watanabe et al. 2003) and Dome C (EPICA-community-members 2004) and almost a full climatic cycle in Greenland at Summit (Cuffey and Clow 1997; Johnsen et al. 1997) and even further at NorthGRIP (NorthGRIP-community-members 2004).

The progressive distillation of air masses during the moisture advection from mid to high latitudes is classically used to estimate past temperature changes from polar ice core water isotopic composition in either $\delta^{18}O$ or δD (Dansgaard 1964; Lorius et al. 1969). This "isotopic thermometer" can however be biased by past changes in snowfall seasonal deposition (Krinner et al. 1997; Werner et al. 2000); moisture origin (e.g. Boyle 1997; Cuffey and Vimeux 2001a, b) or other factors (inversion strength, short term covariance between precipitation and temperature...). The full isotopic composition of snow and ice itself brings constraints on changes in moisture origin, owing to the deuterium excess parameter ($d = \delta D - 8\ \delta^{18}O$) (Masson-Delmotte et al. 2005a, b; Stenni et al. 2001). Climate models are useful tools to help estimate past changes in deposition conditions (seasonal cycle of precipitation, condensation temperature versus surface temperature) which may alter the water stable isotope to temperature relationships.

In Antarctica, water stable isotopes only have been used to quantify glacial-interglacial temperature changes. The consistency of ice core dating with an ice flow model fed by the temperature and accumulation derived from water stable isotope fluctuations warrants the realism of these reconstructions, within 20–30% (Jouzel et al. 2003; Parrenin et al. 2001; Stenni et al. 2001; Watanabe et al. 2003). LGM to present surface air temperature change is estimated to be $9 \pm 2°C$; this error bar is estimated by modelling of precipitation isotopic composition changes with an air mass distillation model, taking into account changes in moisture origin derived from measurements of deuterium excess in the ice (Jouzel et al. 2003; Stenni et al. 2001; Watanabe et al. 2003). This temperature change may partly arise from an ice sheet elevation difference between modern and glacial conditions, with variable ranges of estimates (Ritz et al. 2001; Peltier 2004). Such elevation effects may also partly influence local Antarctic MH temperature change; most inland ice core isotopic records suggest that MH temperatures were either similar or warmer by at most 0.8°C (Masson et al. 2000). A few coastal records such as Taylor Dome or Law Dome suggest that MH temperatures could have been warmer by more than 1°C (Steig et al. 1998).

Although associated with 20–30% uncertainty in Antarctica, temperatures derived from water stable isotope measurements in Greenland have been showed to underestimate glacial temperature changes in Greenland. Alternative paleothermometry methods have been developed and are particularly suited for Greenland where the accumulation rate is typically two to ten times larger than for central Antarctica. Precise measurements of the vertical temperature profiles in the boreholes when the drilling operations are completed provide direct reconstructions of past temperatures owing to the heat diffusion in ice sheets. However, the inversion of the heat diffusion equations requires a priori knowledge of the shape of the temperature variations so there are still uncertainties on MH and LGM changes, typically within 2°C (Cuffey et al. 1995; Johnsen et al. 1995; Cuffey and Clow 1997; Dahl-Jensen et al. 1998). These borehole temperature reconstructions show that MH temperatures were typically 1.5–2.5°C warmer than now and LGM temperatures 19–22°C colder than now. By contrast, temperature reconstructions based on water stable isotopes suggest a smaller MH warming (0.5–0.9°C) (Masson-Delmotte et al. 2005a, b) and only a 10°C amplitude for the glacial interglacial change. This can only be reconciled with the LGM borehole temperature profile when taking into account dramatic changes in the precipitation seasonal cycle: the lack of winter snowfall during glacial times, in response to changes in sea–ice and land–ice cover, could be responsible for a seasonal bias as suggested by simulations conducted with atmospheric general circulation models (Krinner et al. 1997; Krinner and Werner 2003; Werner et al. 2000).

Although obtained at individual locations, the most reliable ice core based temperature estimates (borehole data for Greenland, stable isotopes for East Antarctica) are representative not only of their local drilling site but of central ice caps, as evidenced by the convergent records from a variety of ice cores (Fig. 1). In the following sections, we compare model results averaged over inland ice caps with these ice core based estimates.

3 Model experimental design

For future climate change we consider the two scenarios where atmospheric CO_2 levels were respectively stabilised at a doubling of pre-industrial levels (hereafter $2\times CO_2$) and a quadrupling of pre-industrial levels (hereafter $4\times CO_2$) after a 1% per year increase from pre-industrial levels. We only consider recent model simulations performed for the IPCC fourth assessment available from the CMIP database. In these two cases, we have calculated the difference between a 50-year period of the stabilisation period (centred on the time period of 75 years after the end of atmospheric CO_2 increase) and a 50-year period of the control run

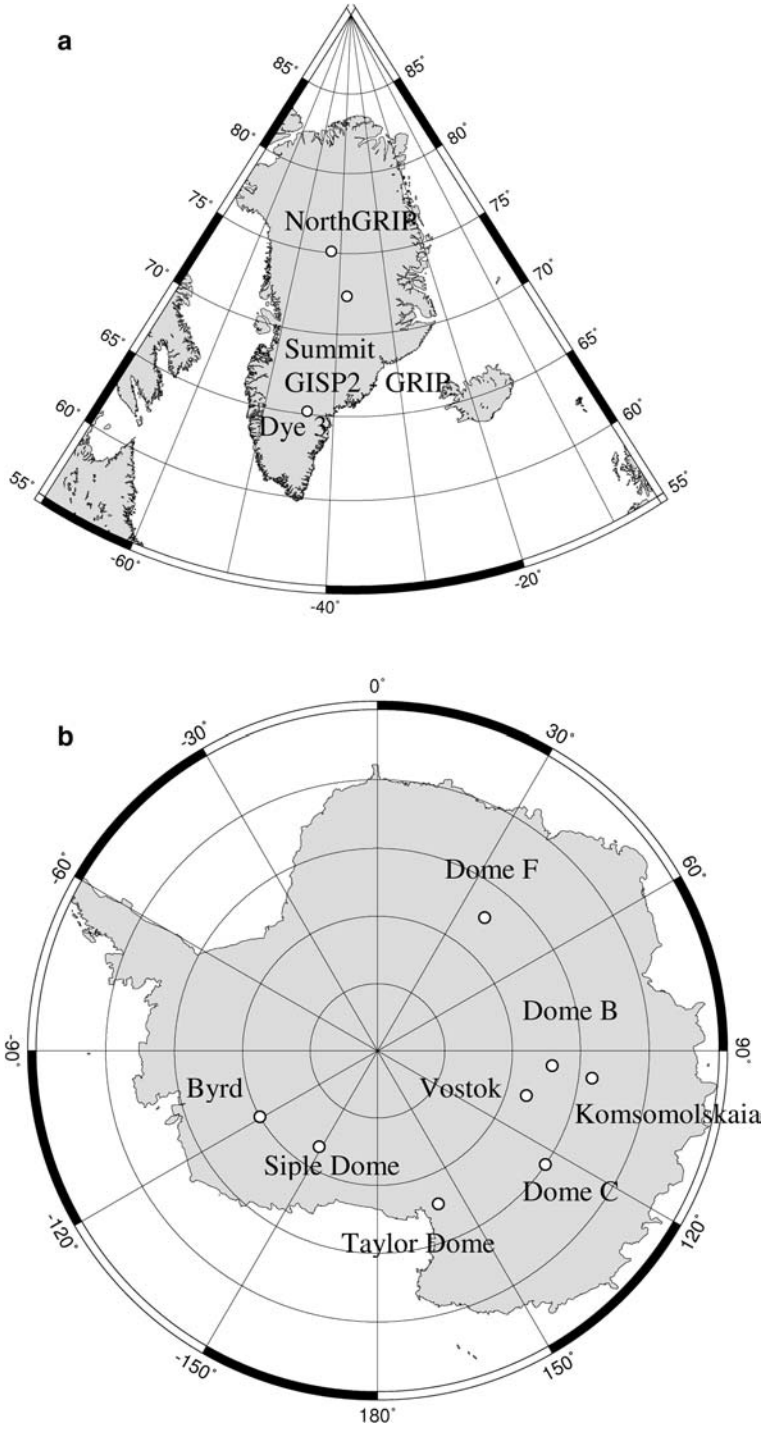

Fig. 1 Maps showing the location of ice core records used to infer estimates of LGM temperature changes in **a** Greenland and **b** Antarctica. From south to north, in Greenland, *open circles* locate the sites of Dye 3, Summit (GRIP and GISP2) and NorthGRIP ice cores. In Antarctica, from 90°W in the trigonometric directions, *open circles* correspond to Byrd, Siple Dome, Taylor Dome, Dome C, Vostok, Komsomolskaia, Dome B and Dome F ice cores

(Table 1). For a consistent comparison with the paleoclimate results, we need to compute the response of the climate models closest to the equilibrium response, while keeping a maximum of models for our analysis. A set of ten model results was available for the $2\times CO_2$ experiment (nine for the $4\times CO_2$ experiment), including several simulations conducted either with different initial conditions or different model versions from the same groups (Table 2).

For past climates, we have used simulations performed with the same coupled model (''cpl'') versions used in CMIP, as part of PMIP2, with a total of seven models for MH and five for LGM. Earlier simulations conducted with three coupled models but with forcings different from the standard protocol of PMIP2 have also been included (post-PMIP1) (Table 1). In addition, we have also considered atmospheric alone simulations (''fix'') of the first phase of PMIP (16 models for MH and

Table 2 List of simulations and model versions used for this intercomparison

Model name in the database	PMIP1 MH Fixed SST	PMIP2 MH Coupled models	PMIP1 LGM Fixed SST	PMIP1 LGM Calculated SST	Post-PMIP1 LGM Coupled models	PMIP2 LGM Coupled models	CMIP 2×CO2 Coupled models	CMIP 4× CO2 Coupled models
bmrc	X							
ccc2.0	X		X	X				
ccm1				X				
ccm3	X							
ccsr1	X		X					
csiro	X							
climber-2				X				
cnrm-2	X							
echam3	X		X					
gfdl	X			X				
gen1				X				
giss-iip	X							
lmcelmd4	X		X	X				
lmcelmd5	X		X					
mri2	X		X	X				
ugamp	X		X	X				
uiuc11	X							
ukmo	X			X				
yonu	X							
MIROC3.2 (medres)		X				X	X	X
NCAR_CCSM3		X				X	X	X
FOAM		X						
IPSL-CM4-V1-MR		X				X	X	X
UBRIS-HADCM3M2		X OA and OAV						
GISSmodelE-R		X					X	
UKMO-HADCM3M2						X		
ECBILTCLIO						X		
MRI-CGCM1					X			
HADCM3					X			
UToronto-CCSM1.4					X			
CNRM-CM3							X	
GFDL-CM2.0							X	X
GFDL-CM2.1							X	X
GISS-EH							X	
GISS-ER							X	X
FGOALS-g1.0		X				X	X (3 simulations)	
INM-CM3.0							X	X
ECHAM5/MPI-OM							X	X
MRI-CGCM2.3.2							X	X (2 simulations)
Number of simulations	16	8	7	9	3	4	16	11

For the description of the different models please refer to the CMIP and PMIP databases descriptions (http://www.lsce.cea.fr/pmip/, http://www.lsce.cea.fr/pmip2/, http://www.pcmdi.llnl.gov/ipcc/about_ipcc.php)

7 for LGM) as well as nine atmospheric models coupled with slab ocean models (''cal'') for LGM (Tables 1, 2). The ''fix'' and ''cal'' PMIP runs are equilibrium simulations and all years of simulated climate available in the database were averaged (Table 1); for PMIP2, modelling groups provided 30 to 100 year long outputs, obtained after major adjustments to the forcings (but without constraints on deep ocean equilibrium). These 100 year long outputs where averaged for our analyses.

The most recent simulations (CMIP and PMIP2) use coupled ocean–atmosphere models and their reference simulations are long pre-industrial control runs. In the case of PMIP1 atmosphere and atmosphere with slab ocean models, the reference simulation is the modern climate. In between these two standardized procedures, post-PMIP1 simulations used either modern or pre-industrial reference simulations; these differences are not critical for our analyses.

We have extracted from the CMIP, PMIP1 and PMIP2 databases the available monthly model outputs (temperature, orography and for the paleoclimate simulations also precipitation). In all the figures and the rest of this paper, all the temperature anomalies will be discussed as control minus LGM, control minus MH, and $2\times CO_2$ or $4\times CO_2$ climate minus control climate, for consistency of time direction. Global and regional results were calculated by weighting each model grid point by the actual area of these grid points. For each available simulation, we have calculated the global mean temperature change. For each model, Central Greenland was defined as the model grid points located between 65 and 80°N, 60 and 25°W, with an elevation above 1,300 m. The same approach was used for Central Antarctica with grid points between 90 and 70°S, 0 and 180°E, and an elevation above 2,500 m.

4 Results and discussion

4.1 Model-data comparisons: preliminary remarks

4.1.1 Last glacial maximum ice cap elevations

The representation of the orography in atmospheric models strongly depends on their resolution and their discretisation method (spectral or grid-point). The average control run central Greenland orography varies between 1,315 and 2,376 m. This dispersion could explain the large range of model results for the control simulation. We therefore do not compare absolute values for each period but anomalies with respect to the control runs.

The ICE-4G LGM ice cap prescribed in PMIP1 and post-PMIP1 (Peltier 1994) is characterized by an average 800 m elevation increase compared to the present altitude (between 640 and 924 m). In contrast, the ICE-5G LGM ice cap reconstruction prescribed for the PMIP2 simulations (Peltier 2004) have a much reduced central Greenland elevation anomaly (106–275 m). However, both ice-core air content information (Raynaud et al. 1997) and ice sheet modelling (Tarasov and Peltier 2003) suggest that changes in central Greenland elevation were limited (and even in the opposite direction). We therefore face the problem that different LGM simulations were conducted with different glacial Greenland elevation changes, significantly larger than those derived from ice core information and ice sheet modelling. When considering the typical polar vertical temperature lapse rate (circa 10°C per 1,000 m) (Krinner and Genthon, 1999), such discrepancies in elevation changes (up to 800 m) may account for up to 8°C temperature differences (without taking into account atmospheric dynamics related to glacial ice cap topographies).

In central Antarctica, the modern elevation represented in the models varies between 2,956 and 3,448 m. For PMIP1, the prescribed ice sheet change (Peltier 1994) results in an average elevation increase of 368 m (from 120 to 430 m depending on the models). For post-PMIP1, all the models analysed here show changes of elevation between 392 and 399 m. For PMIP2 with the ICE-5G ice caps, similar orders of magnitude are also obtained (Peltier 2004) (elevation changes ranging between 343 and 400 m above modern levels). Again, this central Antarctic ice cap elevation increase at the LGM is too high when compared with ice core air content changes or with dynamical ice cap modelling forced by ice-core based climate histories (Ritz et al. 2001).

Because of the hundreds of meters of maximum differences both in modern polar elevations and in LGM to modern changes, we have compared model outputs directly, as well as with a correction for changes in elevation. Observations of modern polar vertical lapse rate and spatial elevation-temperature gradients show lapse rates varying between 6°C per 1,000 m and 15°C per 1,000 m depending on the season and the location (Ohmura and Reeh 1991; Krinner and Genthon 1998, 1999). In order to account for large glacial to modern central ice sheet elevation changes, we have used a constant first order lapse rate of 10°C per 1,000 m. The use of this lapse rate provides a rough estimate of the effect of the prescribed orography changes; we estimate that this elevation correction is associated with a maximum uncertainty of 50%, given the range of observed modern polar lapse rates.

For reference, we have applied this methodology to compare the control simulations (Table 1) with the modern temperatures at deep ice core sites. The range of control simulation elevations are displayed together with temperatures ''uplifted'' at the elevation of ice core sites (typically 3,000 m for central Greenland and 3,400 m for East Antarctic Plateau). It can be observed that, in average, climate models capture the correct expected range of elevation-corrected temperatures in central Greenland. By contrast, there is a tendency to observe an underestimation of elevation-corrected temperatures on the East Antarctic Plateau by a few degrees (Table 3); this may be due to different representations of the Antarctic inversion strength.

Table 3 « Central Greenland » and « East Antarctic Plateau » control simulations of elevation and temperature respectively uplifted to 3,000 and 3,400 m elevation (taking into account a vertical lapse rate of 10°C per 1,000 m)

Control runs for experiments	Central Greenland corrected temperature ("uplifted" at 3,000 m elevation, °C)	Central Greenland elevation (m)	East Antarctic Plateau corrected temperature ("uplifted" at 3,400 m elevation, °C)	East Antarctic Plateau simulated / observed elevation (m)
PMIP1 6fix	−29.6 ± 5.7	1,921 ± 239	−47.3 ± 8.0	3,095 ± 120
PMIP1 21 fix	−28.4 ± 8.2	1,942 ± 321	−44.8 ± 10.1	3071 ± 70
PMIP1 21 cal	−30.5 ± 4.3	1,899 ± 189	−45.3 ± 7.6	3,115 ± 85
Pre-PMIP2	−32.9 ± 5.4	1,835 ± 212	−49.5 ± 7.2	3,059 ± 30
PMIP2 6 k cpl	−34.1 ± 2.9	1,826 ± 152	−50.3 ± 3.0	3,053 ± 72
PMIP2 21 k cpl	−33.5 ± 3.4	1,883 ± 233	−48.9 ± 5.5	3,057 ± 71
IPCC 2×CO2	−32.1 ± 2.9	2,007 ± 144	−48.7 ± 2.7	3,050 ± 41
IPCC 4×CO2	−32.0 ± 3.2	2,005 ± 150	−50.4 ± 2.5	3,065 ± 24
GRIP	−29.7	3,200		
NorthGRIP	−32.4	2,917		
Vostok			−54.6	3,490
Dome C			−55.5	3,200
Dome B			−55.0	3,650
Komsomolskaia			−51.6	3,500

For comparison, mean characteristics of various drilling sites (see Fig. 1) are also displayed. Uncertainties in the vertical lapse rate used for elevation corrections should induce uncertainties on corrected temperatures within 1–2°C. For each type of control simulation, the mean value of all model outputs available is displayed together with the inter-model standard deviation

4.1.2 Comparing model outputs with ice core isotope paleothermometry

Water stable isotopes record past temperature changes through the progressive depletion of atmospheric vapour of heavy molecules along their transport path from moisture sources to the poles. The relationship between isotopic composition and temperature therefore results from the control of cloud temperature on condensation. Changes in moisture source origin, in the gradient between surface and condensation temperatures may induce changes in the temporal relationships between polar precipitation isotopic composition and temperature. Deuterium excess data from both poles suggest that changes in moisture source is not a major bias on glacial interglacial ice core based temperature reconstructions (Cuffey and Vimeux 2001a, b; Stenni et al. 2003, 2001). By contrast, changes in the seasonal cycle of precipitation remain one plausible explanation for the mismatch between Greenland glacial temperature change derived from borehole measurements versus temperature derived from the classical spatial isotope/temperature slope (Masson-Delmotte et al. 2005, b). In the present work, we have not assessed changes in the vertical temperature gradient, some of the databases which we use missing this type of data. However, we have attempted to estimate the impact of precipitation seasonality changes on past temperatures recorded in ice cores. For this purpose, we have taken into account the impact of changes in the seasonal cycle of the precipitation by comparing the change in annual mean temperature (arithmetic average of 12 monthly mean temperatures) with the change in precipitation-weighted annual mean temperature, for each LGM simulation (calculated from monthly outputs of temperature and precipitation; Fig. 4a, b), following the methodology of (Krinner et al. 1997; Krinner and Werner 2003; Werner et al. 2001). When calculated from all the control simulations available, this seasonality effect accounts for a 2.3 ± 1.7 and 3.3 ± 2.9°C difference between the modern precipitation weighted temperatures and the annual mean temperatures, respectively for Greenland and East Antarctica. This is the consequence from the fact that climate models simulate slightly more precipitation today during the warmest months in both polar regions than during the coldest months; this effect is reinforced at the LGM. Indeed, PMIP2 results show systematic shifts towards more precipitation provided during the warm season at LGM. If this change of seasonal cycle is real, this effect may account for an underestimation of LGM annual mean temperature changes as recorded in stable isotopes from ice cores, which remains however limited. The differences between weighted LGM and annual mean LGM temperatures increase to 4.0 ± 0.8 and 4.6 ± 1.3°C for Greenland and Antarctica, accounting for a relative uncertainty of 8–23% of the full glacial-control range, depending on the hemisphere and on the model.

4.2 Global mean temperature changes

In order to assess the range of global temperature changes simulated by climate models under 2×CO_2, 4×CO_2, MH and LGM boundary conditions, we have compared on Fig. 2 the distribution statistics (full range, 25th, 50th, 75th quartiles and the mean of all models) of model results for these various experiments. This presentation is well suited when limited numbers of simulations are available (in our case from 4 to 16) and helps visualizing the range (maximum to minimum values), the average, median and dispersion of model results. In particular, extrema levels significantly different from the

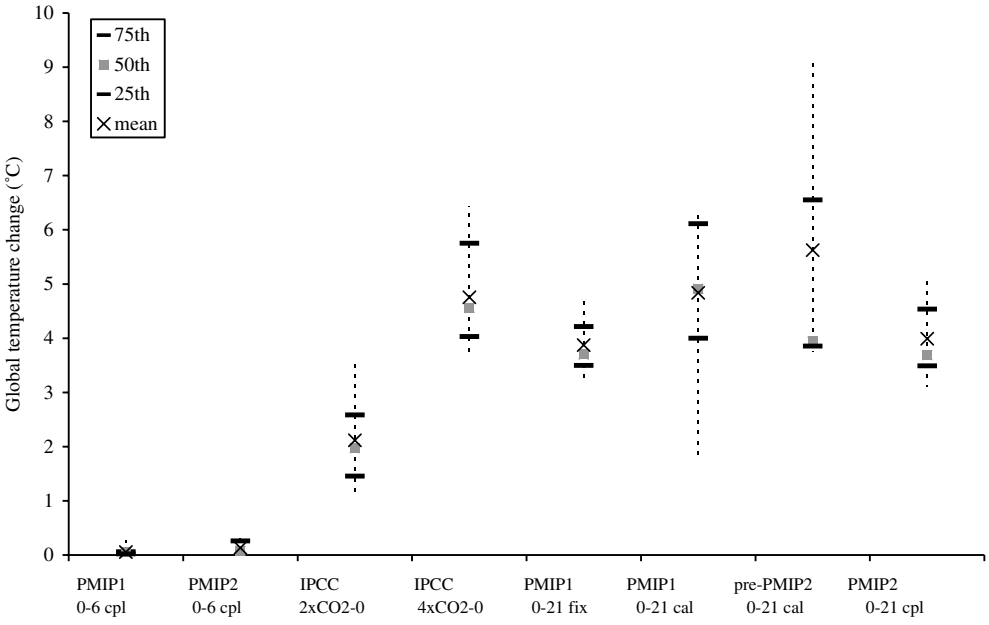

Fig. 2 Annual mean global temperature changes simulated by a variety of climate models run under similar boundary conditions. The full range (*dashed line*), mean (*cross symbol*), 25th (*lower bold dash symbol*), 50th (*grey square symbol*), 75th (*upper bold dash symbol*) percentiles of the various model results are calculated from the distribution of the various model results (see Table 2). The "fix", "slab" and "cpl" abbreviations refer to different configurations of models used and are described in Sect. 3 and Table 1

25th to 75th ranges clearly identify the occurrence of outliers among the different model results.

For the MH, 6,000 years ago, climate models do capture reconstructed seasonal and regional changes such as wetter conditions in northern Africa (Joussaume et al. 1999; Braconnot et al. 1999) or warmer conditions in some areas of the mid-latitudes in summer (Cheddadi et al. 1997; Masson et al. 1999; Wohlfahrt et al. 2004). This results from a seasonal and latitudinal redistribution of solar radiative forcing due to changes in precession and obliquity of the Earth's orbit (Berger 1978; Joussaume and Braconnot 1997) modulated by the differential heat capacity of the ocean and land masses as well as by the sea–ice response at high latitudes (Crucifix et al. 2002). In some regions, the seasonal changes do have a signature in the annual mean; this is for instance the case for annual mean precipitation in monsoon regions. Globally, the mean temperature change between control and MH simulations is between −0.05 to +0.4°C with a median value of respectively +0.05 and +0.08°C for PMIP1 atmospheric models and PMIP2 coupled climate models. In average, climate models simulate slightly warmer control global temperatures compared to the MH simulations (Fig. 2). Note that in this MH case, when global mean temperature changes are small, the notion of global climate sensitivity computed from global and annual averages is not suitable because it does not account for the seasonal aspects both in terms of orbital forcing and climate response.

The median range of control minus LGM global temperature change is fairly constant for PMIP1 simulations conducted with CLIMAP ocean surface boundary conditions ("fix") and atmospheric models alone, PMIP1 simulations with atmospheric models coupled with mixed layer ocean models ("cal") and PMIP2 simulations with fully coupled ocean-atmosphere climate models ("cpl"). The median of model results is rather stable from PMIP1 to PMIP2 (3.7°C for fixed SST, 4.9°C for calculated SST, 3.9°C for post-PMIP1 and 4.1°C for PMIP2 results). With the exception of two outliers (LMCELMD4 for PMIP1 cal and UTORONTO-CCSM1.4 for post-PMIP1), all model results range between 3.1 and 6.4°C in terms of glacial to control global temperature change

The range of global temperature change for $4\times CO_2$ experiments, with a median of 4.3°C, is comparable to the LGM to modern change. In the case of $2\times CO_2$ experiments, the global temperature range has a median of 2.0°C. The dispersion range between various model results (indicated by the vertical dashed line in Fig. 2) is significant when compared to the full amplitude of the changes. In the case of future climate change scenarios, climate models have a range of dispersion of the same order of magnitude as the median change: 2.3°C for $2\times CO_2$ and 2.7°C for $4\times CO_2$. A similar 2°C dispersion is also observed for PMIP2 LGM to modern changes. The difference among individual models forced with similar boundary conditions is therefore about 100% of the median global temperature change in the case of $2\times CO_2$, and 50% of the median global temperature change in the case of $4\times CO_2$ and LGM simulations.

This comparison shows that the global temperature response is very similar under $4\times CO_2$ and LGM forcings, although occurring in response to different spatially-distributed forcings (greenhouse gases in one case, greenhouse gases plus ice sheets in the other case).

4.3 The particular case of MH polar temperature change: model-data comparison

For the MH, it is impossible to discuss a polar amplification of climate change, defined as the ratio between

the temperature change in central polar regions to global temperature changes, due to the negligible global mean temperature changes.

For central Greenland, simulations conducted with fixed ocean surface conditions within PMIP1 show a large dispersion of temperature change between MH and control conditions (range between −0.8 and 1.5°C with half of the models simulating warmer and half of the models simulating colder conditions than present). This dispersion is probably related to different responses of the atmospheric stationary waves and the associated heat transport to Greenland; note that the range of temperature changes is quite small compared to the typical temperature interannual variability range (Masson et al. 1998). By contrast, all the PMIP2 coupled model simulations performed with an interactive ocean and sea–ice model simulate a temperature decrease from MH to modern conditions varying from 0.35 to 0.90°C, consistent with paleoclimatic estimates of warmer MH conditions, but weaker than borehole temperature reconstructions (Dahl-Jensen et al. 1998; Masson-Delmotte et al. 2005a, b). The use of fully coupled climate models therefore improves the consistency of the model results over Greenland. Indeed, coupled climate model simulate a shaping of the seasonal cycle by the ocean response associated with a late summer warming, a reduced sea–ice cover and an Arctic warming (Vavrus and Harrison 2003). Although PMIP2 models do capture the correct sign of the reconstructed temperature change, they underestimate the amplitude of the MH Greenland temperature change in average by a factor of 3. Last, these simulations enable us to explore changes in the precipitation seasonal cycle as a clue to reconcile borehole and water isotope temperature reconstructions. All the PMIP2 MH simulations reveal that precipitation-weighted temperature changes should be larger than the arithmetic annual mean of monthly temperatures, resulting in a range of precipitation-weighted temperature changes from 1.0 to 1.2°C (due to more snowfall during the warmest months). This is not consistent with the different ranges of temperature changes estimated from borehole versus stable isotope thermometry, and further suggests that the change in moisture advection simulated by PMIP2 coupled models may not be correct. It has to be noted that the PMIP2 simulations did not systematically include changes in vegetation. Earlier studies had shown that changes in high northern latitude vegetation enhanced the local warming (Wohlfahrt et al. 2004).

We have performed the same analysis of MH model results for central Antarctica. PMIP1 simulations show no model consistency and result in changes in Antarctic temperatures varying from −0.6 to +0.7°C. Again, PMIP2 simulations performed with coupled models systematically show a temperature decrease from MH to modern levels, by 0.1–0.7°C. As for Greenland, this larger consistency among models is attributed to seasonal ocean and sea–ice response in the surrounding areas. For central Antarctica, coupled models are qualitatively and quantitatively in agreement with temperature reconstructions based on water isotopes from polar ice cores, which suggest a range of temperature change from 0 to +0.8°C (Masson et al. 2000). When precipitation seasonality is considered, the simulated temperature range shifts by 0.3–0.6°C, confirming the previous range of temperature change and furthermore the fact that changes of Antarctic precipitation seasonal cycle should not be a major source of uncertainty when reconstructing local past temperature changes from ice core water stable isotopes, even within the current interglacial period (Jouzel et al. 2003).

4.4 Polar amplification: LGM versus future climate simulations

Here we discuss the ratio of polar versus global mean temperature changes. Figure 3a displays the comparison of LGM and future climate change range of model results for CMIP and PMIP1 and PMIP2 intercomparison exercises. Increasing CO_2 concentrations imposed in $2\times CO_2$ and $4\times CO_2$ induce a central Greenland temperature change of respectively 1.37 and 1.40 times above the simulated global temperature increase; in central Antarctica, this amplification factor is respectively 1.16 and 1.25. This intercomparison therefore confirms previous studies conducted as a function of latitude but only for the northern hemisphere (Holland and Bitz 2003). Because the median of all climate models is systematically above 1 (Fig. 3), we can reasonably argue that both past and future climate changes are indeed associated with a polar amplification of climate change.

For the LGM, part of this polar amplification may be due to the local elevation increase imposed by ice sheet reconstructions used as boundary conditions (Peltier 1994, 2004) (see Sect. 4.1.1). In order to assess the proportion of local temperature changes which could be accounted for by local topography changes, we have added "elevation corrected" results where LGM simulated temperature changes are corrected from changes in elevation using a slope of 10°C per 1,000 m elevation (these calculations appear as "corr" labels in Fig. 3).

Glacial boundary conditions induce a very large polar amplification for Greenland (Fig. 3a). PMIP1 boundary conditions result in a factor of 5 between Greenland and global temperature changes, and a factor of 3 when corrected for large elevation changes. Such a large amplification is clearly the result of the imposed CLIMAP surface conditions (including a large sea–ice coverage in the North Atlantic plus rather warm tropical temperatures). By contrast, PMIP2 simulations conducted with a different ice sheet topography (Peltier 2004) and with fully coupled ocean–atmosphere–sea ice models suggest a range of amplification of 2.6–2.1 (respectively without and with topography correction) (Fig. 4a). These results suggest

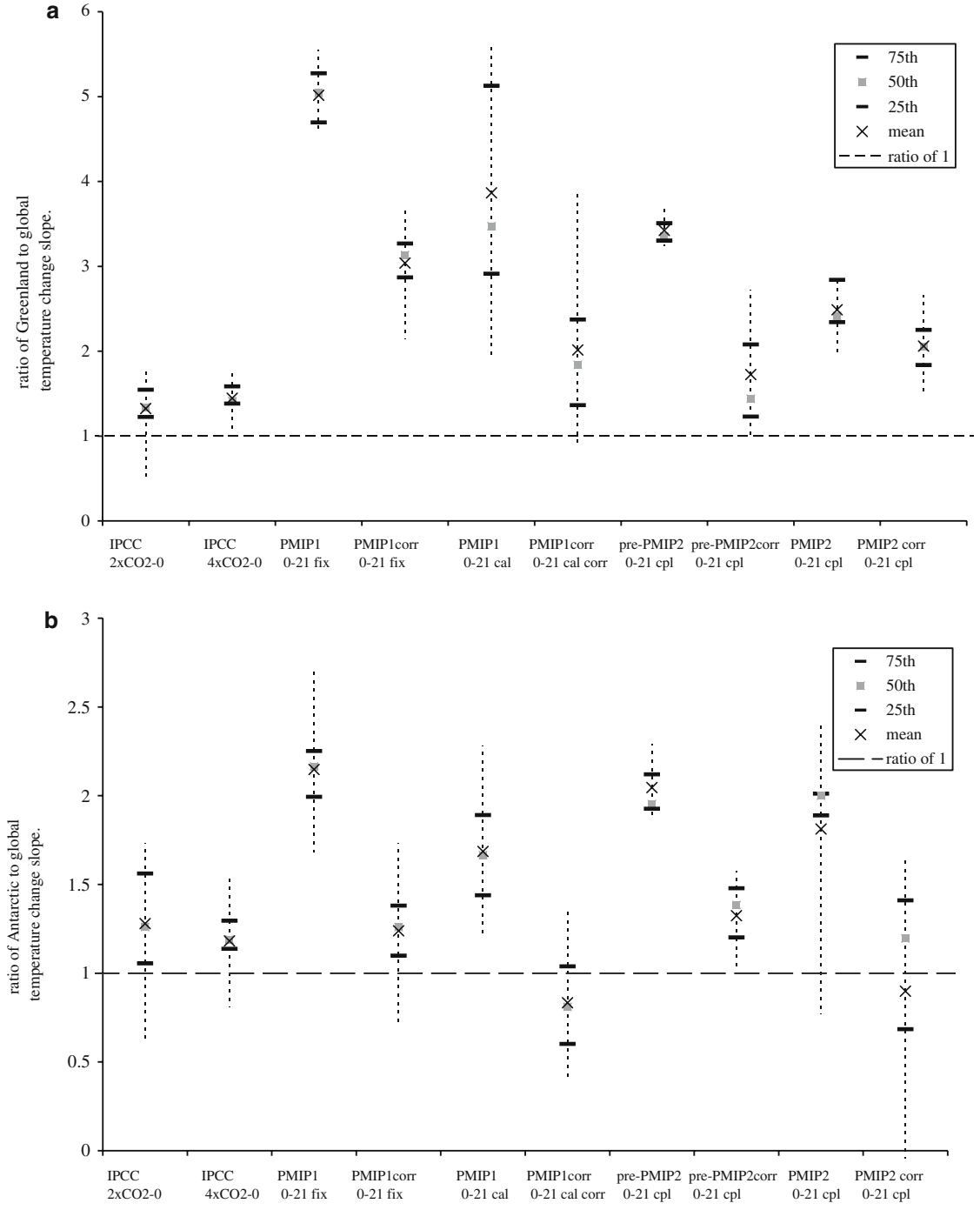

Fig. 3 **a** Central Greenland polar amplification (defined as the ratio between central Greenland and global annual mean temperature changes) simulated by climate models. The full range (*dashed line*), mean (*cross symbol*), 25th (*lower bold dash symbol*), 50th (*grey square symbol*), 75th (*upper bold dash symbol*) percentiles of the various model results are calculated from the distribution of the various model results (see Table 2). "corr" stands for elevation-corrected temperature values (see text). **b** Same as (**a**) but for central eastern Antarctica. Note that the vertical scale is half as small as for Greenland

that Greenland temperature changes are deeply amplified under glacial conditions, due to (1) imposed local topography changes (up to half of the signal), (2) northern hemisphere albedo, atmospheric and ocean circulation effects. The impact of large sea–ice changes in the North Atlantic on Greenland temperature is most obvious from the dispersion of PMIP1 slab ocean simulations. Many of these processes should be active both in the warming from glacial to modern conditions and in the warming from modern to future conditions. Note that future climate change simulations analysed here do not account for the possible polar ice sheet

response in terms of elevation change. Preliminary results obtained with an earth climate model of intermediate complexity fully coupled to Greenland and Antarctica ice-sheet models (S. Charbit et al., personal communication) suggest that such effects should be important for central Greenland, similar to the findings of (Huybrechts et al. 2004).

In Central Antarctica (Fig. 3b), the range of polar amplification is smaller than for central Greenland both for future and glacial climate changes; this is probably due to the larger albedo effect in the northern hemisphere due to ice caps and snow cover over the continents, and to changes in northern hemisphere storm tracks. PMIP1 boundary conditions result in an amplification factor of 2.1 (without orography correction) to 1.2 (with orography correction). PMIP2 simulations conducted with coupled climate models give rather similar ranges of changes (median model amplification factors of respectively 1.9 and 1.2). The sea–ice changes simulated by PMIP1 slab ocean runs, post-PMIP1 and PMIP2 models is systematically less extensive than previously prescribed from CLIMAP reconstructions, consistent with new austral sea–ice reconstruction efforts (Gersonde et al. 2005). When orography effects on central Antarctic temperature changes are roughly accounted for (Fig. 4b), the order of magnitude of polar amplification are very comparable to the range of future Antarctic amplification (around 1.20); some models even show no Antarctic amplification. The coherency of Antarctic temperature change with global temperature change may result from a dominant role of greenhouse gases on southern high latitude radiative budget, only slightly modulated by the internal feedbacks associated with sea–ice extent, cloudiness, atmospheric heat and moisture advection (including water vapour feedback, more important at high latitudes). By contrast, we can speculate that Greenland polar amplification should be more influenced by other processes such as dust forcing, changes in vegetation in the northern mid and high latitudes, large icy surfaces and associated feedbacks on atmospheric circulation and heat transport to Greenland.

4.5 Ice-core constraints on global temperature changes

When taking into account all available $2\times CO_2$ and $4\times CO_2$ simulations, a linear regression relating Greenland to global temperature change leads to a slope of 1.46 and a determination coefficient (R^2) of 0.9 (Fig. 4c). Therefore, in the world of model results, in average, future changes in Greenland temperature are linearly determined by the global temperature range (''climate sensitivity'') but amplified by a factor of 46% (''polar amplification'').

When considering glacial to control climate changes, we restrict here our analysis to the coupled model simulations performed under the same boundary conditions and with models involved in the IPCC fourth assessment (PMIP2 simulations). In this case, central Greenland temperature change is also linearly related to global temperature change with a slope of 2.71 (without topography correction) and a determination coefficient of 0.81 (Fig. 4a). This suggests that paleoclimatic polar temperature reconstruction provide a quantitative constraint on the range of global temperature change. In fact, the range of simulated central Greenland temperature changes lies between 6.2 and 14.5°C, significantly below the borehole temperature estimates of 19–22°C for 21,000 years before present. As for the MH climate, coupled model results do capture the glacial cooling but underestimate by a factor from 1.3 to 3.5 the reconstructed temperature change. Part of this inconsistency could be attributed to the uncertainty linked with the effect of increased dust concentrations on climate during glacial times, probably underestimated when taken into account with atmosphere-only models (Werner 2002). Other missing factors include the lack of LGM vegetation (Crowley and Baum 1997) and soil (Poutou 2003) feedbacks, more important in the northern hemisphere but which should be rather limited for Greenland (Crucifix and Hewitt 2005). When extrapolated, this model-data comparison however suggests that the simulations most consistent with the paleoclimatic constraints are associated with large glacial to control global temperature changes (above 4°C) (Fig. 4b). The precipitation seasonality effect remains negligible (within a few °C) compared to the model-data discrepancy, and even acts against any reconciliation of the isotope to the borehole thermometry (all model results give a smaller amplitude of changes when precipitation weighted). The consistency of model results could question the interpretation of proxy records; however, borehole temperature profiles in central Greenland are based on a physical mechanism (diffusion of heat into the ice).

For central Antarctica, a similar analysis can be performed. When a linear regression is performed on all the range of $2\times CO_2$ and $4\times CO_2$ simulations, this leads to a slope of 1.16 and a determination coefficient of 0.80, suggesting again that future Antarctic temperature change is, in the models, related to the global temperature change, and in average amplified by about 16% above the global mean temperature change (Fig. 4d). When applied to PMIP2 last glacial maximum to control results, the same analysis leads to a slope of 2.09 and a smaller determination coefficient of 0.70 (Fig. 4b). This result suggests that Antarctic temperature changes are representative of large scale temperature changes (up to the global scale), with an amplification factor of 2. This is a model confirmation that the early hypothesis of (Genthon et al. 1987) and (Lorius et al. 1990) remains valid. Antarctic glacial–interglacial temperature changes can be considered to constrain global climate sensitivity to greenhouse gases.

The range of simulated glacial to control central Antarctic temperature change varies between 2.4°C for

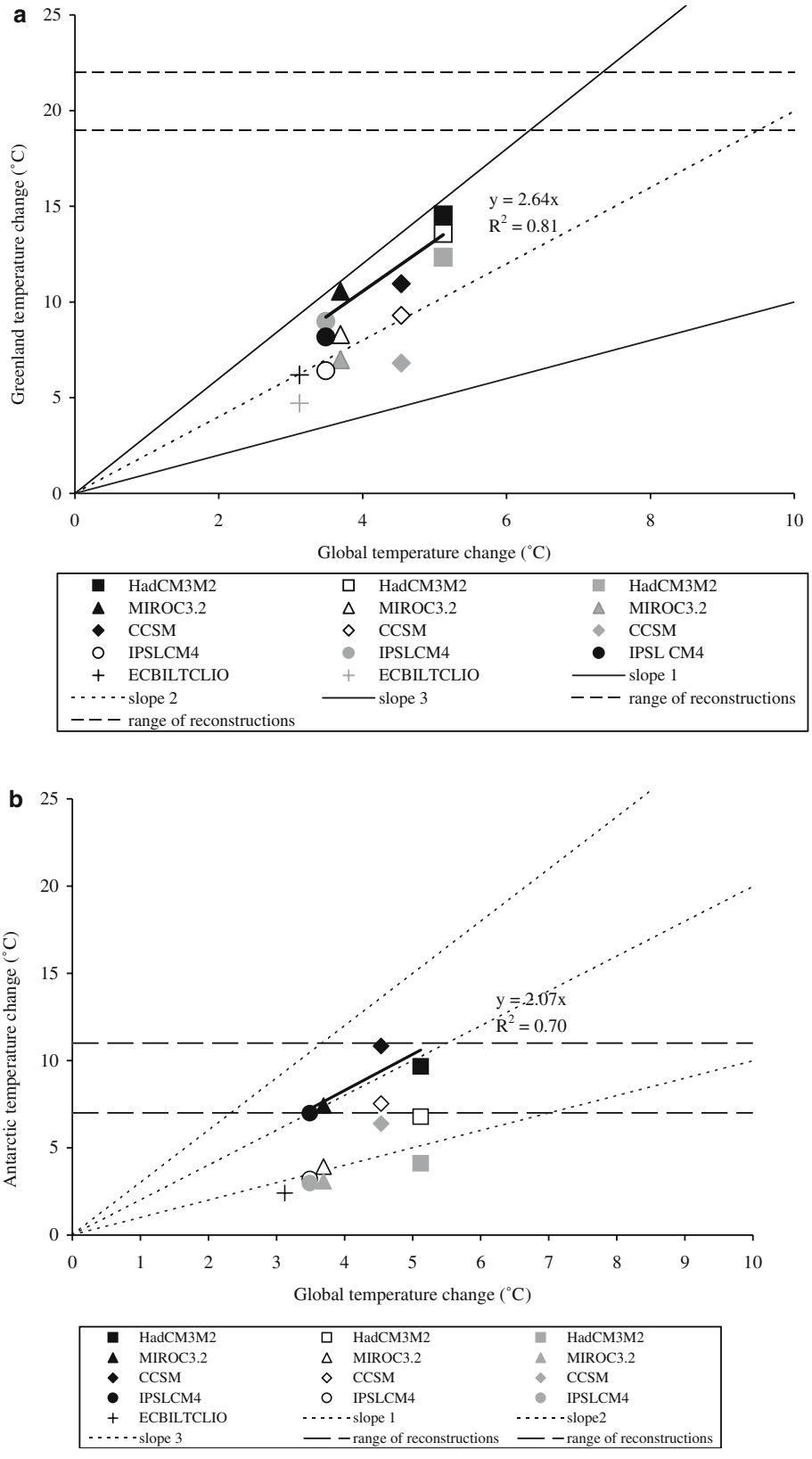

Fig. 4 **a** Comparison of Last Glacial Maximum to control central Greenland annual mean temperature change simulated by climate models (PMIP2 coupled ocean-atmosphere simulations only) with the range of paleoclimatic reconstructions. *Filled black squares* show direct model results. *Open black squares* show model results corrected from LGM to control ice sheet elevation changes ("elevation corrected" results). *Grey squares* show model results corrected from elevation changes and precipitation-weighted ("seasonality corrected" results). *Horizontal long-dashed lines* reflect the range of temperature change derived from Greenland borehole thermometry. *Short-dashed lines* correspond to slopes of 1, 2 and 3 for reference. A linear regression calculated on the results of these four models is also displayed (*solid black line* and regression result). Values below zero are not displayed (results of ECBILT CLIO with corrections. **b** Same as (**a**) but for central Antarctica. *Horizontal long-dashed lines* reflect the range of temperature change derived from Antarctic ice core water stable isotopes. **c** Same as (**a**) but for future climate change simulations. *Open black squares* represent $4\times CO_2$ simulation anomalies, and *filled black rhomboids* $2\times CO_2$ simulation anomalies. The *solid line* is a linear regression on all the simulation results. The *black dashed lines* represent lines with slopes of 1 and 2. **d** Same as (**b**) but for future climate change simulations. *Open black squares* represent 4×CO2 simulation anomalies, and *filled black rhomboids* 2×CO2 simulation anomalies. The *solid line* is a linear regression on all the simulation results. The *black dashed lines* represent lines with slopes of 1 and 2

ECBILT-CLIO (an intermediate complexity climate model) to 10.8°C. The impact of elevation changes accounts for 2.9–3.5°C of the glacial to pre-industrial warming. Without orography correction, all of the four general circulation coupled model results fall within the range of ice-core based temperature range (9 ± 2°C).

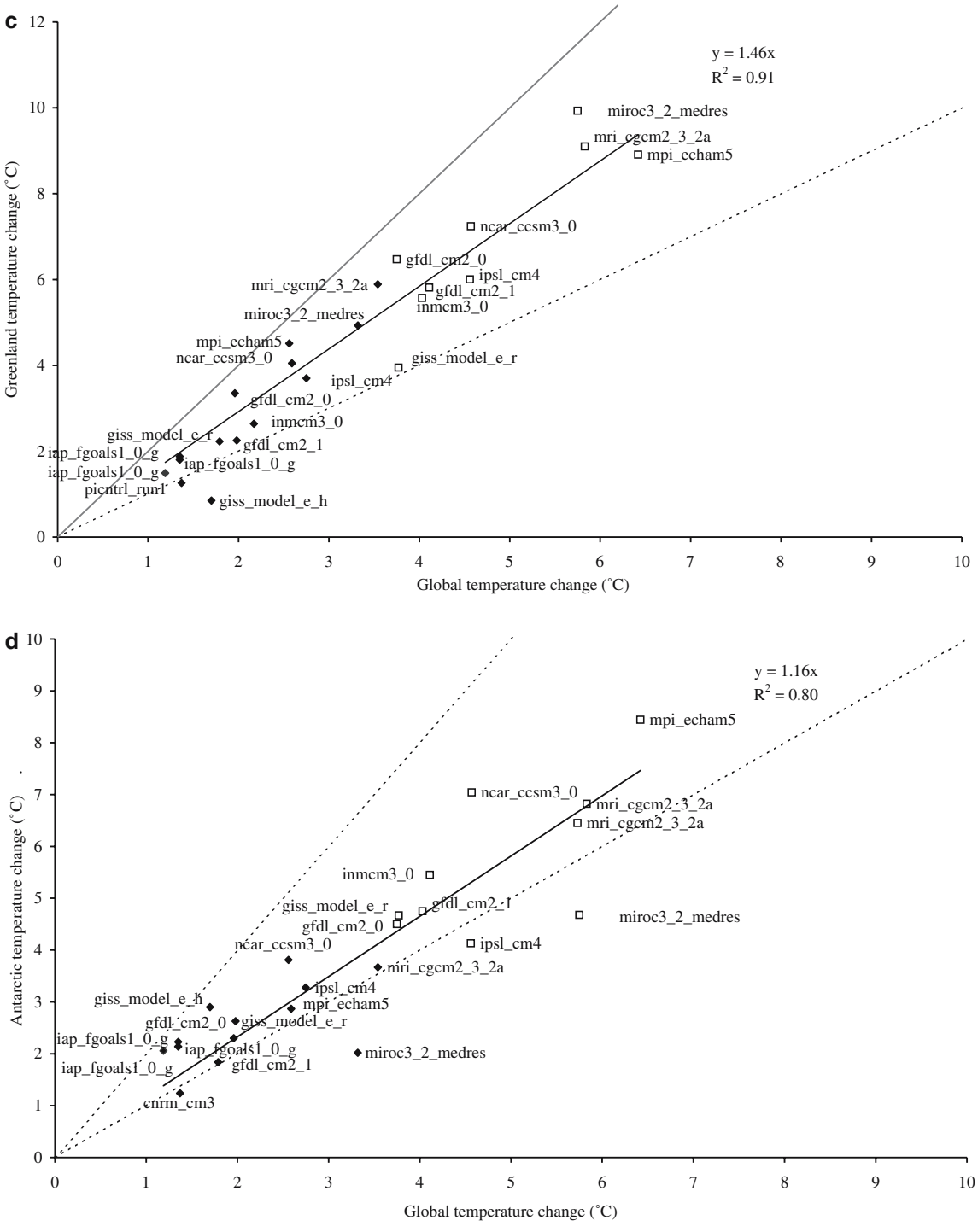

Fig. 4 (Contd.)

This suggests that the range of global glacial to control temperature scale given by these models (3.7–5.1°C) is consistent with the Antarctic proxy data. If the ice sheet elevation change is taken into account, then, again, models do underestimate fixed-elevation central Antarctica LGM temperature change by a factor of 1.2–2.3.

5 Conclusions

We have performed model–model comparisons of past and future climate change at the poles, and model-data comparisons of past polar temperature changes both for the MH and the LGM.

The main outcome of the model–model comparison is that the range of global temperature change is very similar for $4\times CO_2$ experiments and glacial experiments compared to control simulations. The range of inter-model dispersion has the same order of magnitude for glacial and $2\times CO_2$ experiments. Moreover, the polar temperature changes are linearly related to the global temperature change for both future and glacial climate changes, with different polar amplifications at the two poles. In the world of simulated climate change, temperature changes in central Greenland and central Antarctica are therefore representative of global climate sensitivity. The polar amplification in Greenland is much larger than for central Antarctica, possibly due to albedo effects and changes in atmospheric storm tracks.

Paleoclimatic simulations make possible quantitative model-data comparisons with reconstructions based on ice core analyses. For the MH, PMIP1 atmosphere-only models show a large variety of temperature changes. By contrast, coupled climate model simulations performed within PMIP2 all simulate MH temperatures warmer than the control runs in central Greenland and central Antarctica, consistent with ice-core signals, stressing the role of the ocean and sea–ice components of the climate system in integrating the seasonal orbital forcing into an annual mean response. However, they strongly underestimate the amplitude of the central Greenland change, possibly due to the lack of vegetation feedbacks. It has to be noted that these MH polar changes occur with a negligible change in global temperatures. Further efforts will be required to assess the validity of ice core temperature reconstructions in terms of larger scale climate change for other interglacial periods.

The model-data comparison for the LGM is hampered by uncertainties of polar ice sheet topography changes. First, the different central Greenland and central Antarctica ice caps prescribed in the PMIP1 (ICE-4G) and PMIP2 (ICE-5G) exercises are a few hundred meters above modern elevations. Second, these prescribed topographies are in contradiction with ice-core based estimates (either from air content indications, or from ice sheet models forced by ice-core climatic signals). In this paper, we have circumvented this difficulty by comparing direct temperature changes and elevation-corrected temperature changes (with an estimated error of 50% in this correction due to the range of observed modern polar lapse rates). We are aware that this first order correction does not take into account atmospheric dynamical aspects related to the full geometry of the prescribed ice caps. These comparisons show that (1) a significant part of the Greenland and Antarctic cooling of the PMIP1 and PMIP2 simulations is caused by the prescribed local elevation increase at the last glacial; (2) when corrected for elevation changes, models strongly underestimate Greenland temperature changes, although they are rather consistent with Antarctic temperature changes. A direct representation of water stable isotopes inside coupled climate models would help to understand the reasons for such inconsistencies, which here are shown not to arise from changes in precipitation seasonal cycle only. The model-data quantitative discrepancy for central Greenland has to be placed in the larger northern hemisphere context and should be related to changes in stationary waves and storm track trajectories. The response of polar ice caps to future climate change may also act as a positive feedback on the polar amplification, not taken into account in the CMIP experiments discussed here.

The comparison of PMIP1 and PMIP2 models clearly shows that changes in ocean surface conditions (in particular sea–ice extent) are strongly involved in past polar amplification. In order to fully exploit the paleoclimatic constraints on climate sensitivity, future work will be needed to disentangle the local radiative perturbation in response to changes in greenhouse gases from the internal feedbacks involving in particular tropical sea surface temperatures (Lea 2004), sea–ice extent and atmospheric circulation.

6 DATABASE access

http://www.lsce.cea.fr/pmip/
http://www.lsce.cea.fr/pmip2/
http://www.pcmdi.llnl.gov/ipcc/about_ipcc.php

Acknowledgments We acknowledge the international modelling groups for providing their data for analysis, the Program for Climate Model Diagnosis and Intercomparison (PCMDI) for collecting and archiving the model data, the JSC/CLIVAR Working Group on Coupled Modelling (WGCM) and their Coupled Model Intercomparison Project (CMIP) and Climate Simulation Panel for organizing the model data analysis activity, and the IPCC WG1 TSU for technical support. The IPCC Data Archive at Lawrence Livermore National Laboratory is supported by the Office of Science, US Department of Energy. This work was funded by the French Project PNEDC IMPAIRS, European Projects EPICA-MIS and MOTIF (EVK2-2001-00263), and stimulated by discussions during the PMIP meeting in Giens, April 2005. This meeting was funded by CNRS, CEA, PAGES and CLIVAR. The participants are thanked for the discussions around this work. Jean-Yves Peterschmitt offered great help with handling the data and producing the graphics. V.M.D. is funded by CEA and M.K. by CNRS. We thank 3 anonymous reviewers for helpful comments. This is LSCE publication 1770.

References

Alexeev VA et al (2005) Polar amplification of surface warming on an aquaplanet in "ghost forcing" experiments without sea ice feedbacks. Clim Dyn 24:655–666

Bengtsson L et al (2004) The early twentieth-century warming on the Arctic—a possible mechanism. J Clim 17:4045–4057

Berger AL (1978) Long-term variations of daily insolation and quaternary climatic change. J Atmos Sci 35:2362–2367

Boyle EA (1997) Cool tropical temperatures shift the global δ^{18}O-T relationship: an explanation for the ice core ?δ^{18}O borehole thermometry conflict? Geophys Res Lett 24:273–276

Braconnot P et al (1999) Synergistic feedbacks from ocean and vegetation on the African monsoon response to mid-Holocene insolation. Geophys Res Lett 26:2481–2484

Cheddadi R et al (1997) The climate of Europe 6000 years ago. Clim Dyn 13:1–10

CLIMAP (1981) Seasonal reconstructions of the Earth's surface at the last glacial maximum. Geol Soc Am Map and Chart Series, MC-36, 18 p
Corell R et al (2004) Impacts of a warming Arctic: Arctic climate impact assessment. Cambridge University Press, Cambridge, p 144
Crowley TJ, SK Baum (1997) Effect of vegetation on an ice-age climate model simulation. J Geophys Res 102:16463–16480
Crucifix M, Hewitt CD (2005) Impact of vegetation changes on the dynamics of the atmosphere at the Last Glacial Maximum. Clim Dyn 25:447–459
Crucifix M et al (2002) Climate evolution during the Holocene: a study with an Earth system model of intermediate complexity. Clim Dyn 19:43–60
Cuffey KM, Clow GD (1997) Temperature, accumulation, and elevation in central Greenland through the last deglacial transition. J Geophys Res 102:26383–26396
Cuffey KM et al (1995) Large Arctic temperature change at the Wisconsin-Holocene glacial transition. Science 270:455–458
Cuffey KM, Vimeux F (2001a) Covariation of carbon dioxide and temperature from the Vostok ice core after deuterium-excess correction. Nature 412(6846):523–527
Cuffey KM, Vimeux F (2001b) Covariation of carbon dioxyde and temperature from the Vostok ice core after deuterium-excess correction. Nature 421:523–527
Dahl-Jensen D et al (1998) Past temperatures directly from the Greenland ice sheet. Science 282:268–271
Dansgaard W (1964) Stable isotopes in precipitation. Tellus 16:436–468
Dixon KW et al (2003) A comparison of climate change simulations produced by two GFDL coupled climate models. Global Planet Change 37:81–102
EPICA-community-members (2004) Eight glacial cycles from an Antarctic ice core. Nature 429:623–628
Genthon C et al (1987) Vostok ice core: climatic response to CO_2 and orbital forcing changes over the last climatic cycle. Nature 329:414–418
Gersonde R et al (2005) Sea-surface temperature and sea ice distribution of the Southern Ocean at the EPILOG Last Glacial Maximum—a circum-Antarctic view based on siliceous microfossil records. Quaternary Sci Rev 24:869–896
Harrison SP et al (2002) Comparison of palaeoclimate simulations enhance confidence in models. EOS Trans 83:447–447
Holland MM, Bitz CM (2003) Polar amplification of climate change in coupled models. Clim Dyn 21:221–232
Huybrechts P et al (2004) Modelling Antarctic and Greenland volume changes during the 20th and 21st centuries forced by GCM time slice integrations. Global Planet Change 42:83–105
IPCC (2001) Climate change 2001: impacts, adaptation and vulnerability–contribution of working group II to the third assessment report of IPCC, Cambridge University Press, UK, p 1000
Jacka TH, Budd WF (1998) Detection of temperature and sea-ice-extent changes in the Antarctic and Southern Ocean. Ann Glaciol 27:553–559
Johnsen SJ et al (1997) The $\delta^{18}O$ record along the Greenland ice core project deep ice core and the problem of possible Eemian climatic instability. J Geophys Res 102:26397–26410
Johnsen SJ et al (1995) Greenland palaeotemperatures derived from GRIP borehole temperature and ice core isotopic profiles. Tellus 47B:624–629
Joussaume S, Braconnot P (1997) Sensitivity of paleoclimate simulation results to the definition of the season. J Geophys Res 102:1943–1956
Joussaume S, Taylor KE(1995) Status of the paleoclimate modeling intercomparison project (PMIP). In: Gates WL (ed) Proceedings of the first international AMIP scientific conference, Monterey, pp 425–430
Joussaume S et al (1999) Monsoon changes for 6000 years ago: Results of 18 simulations from the paleoclimate modeling intercomparison project (PMIP). Geophys Res Lett 26: 859–862
Jouzel J et al (2003) Magnitude of the isotope/temperature scaling for interpretation of central Antarctic ice cores. J Geophys Res 108:1029–1046
Knorr W et al (2005) Long-term sensitivity of soil carbon turnover to warming. Nature 433:298–301
Krabill W et al (2004) Greenland ice sheet: increased coastal thinning. Geophys Res Lett 31:L24402
Krinner G, Genthon C (1998) GCM simulations of the Last Glacial Maximum surface climate of Greenland and Antarctica. Clim Dyn 14:741–758
Krinner G, Genthon C (1999) Altitude dependence of the ice sheet surface climate. Geophys Res Lett 26:2227–2230
Krinner G et al (1997) GCM analysis of local influences on ice core δ signals. Geophys Res Lett 24:2825–2828
Krinner G, Werner M (2003) Impact of precipitation seasonality changes on isotopic signals in polar ice cores. Earth Planet Sci Lett 216:525–538
Lea DW (2004) The 100,000-Yr cycle in tropical SST, greenhouse forcing, and climate sensitivity. J Clim 17:2170–2179
Lorius C et al (1990) Greenhouse warming, climate sensitivity and ice core data. Nature 347:139–145
Lorius C et al (1969) Variation in the mean deuterium content of precipitations in Antarctica. J Geophys Res 74:7027–7031
Manabe S, Broccoli A (1985) A comparison of climate model sensitivity with data from the last glacial maximum. J Atmos Sci 42:2643–2651
Masson-Delmotte V et al (2005a) Deuterium excess reveals millennial and orbital scale fluctuations of Greenland moisture origin. Science 309:118–121
Masson-Delmotte V et al (2005b) Holocene climatic changes in Greenland: different deuterium excess signals at GRIP and NorthGRIP. J Geophys Res 110, Art. No. D14102
Masson V et al (1999) Mid-Holocene climate in Europe: what can we infer from PMIP model-data comparisons? Clim Dyn 15:163–182
Masson V et al (1998) Impact of parameterizations on simulated winter mid-Holocene and Last Glacial Maximum climatic changes in the Northern Hemisphere. J Geophys Res 103:8935–8943
Masson V et al (2000), Holocene climate variability in Antarctica based on 11 ice cores isotopic records. Quaternary Res 54:348–358
Moritz RE, et al. (2002) Dynamics of recent climate change in the Arctic. Science 297:1497–1502
NorthGRIP-community-members (2004) High resolution climate record of the northern hemisphere reaching into last interglacial period. Nature 431:147–151
Ohmura A, Reeh N (1991) New precipitation and accumulation maps for Greenland. J Glaciol 37:140–148
Parrenin F et al (2001) Dating of the Vostok ice core by an inverse method. J Geophys Res 106:31837–31851
Peltier WR (1994) Ice age paleotopography. Science 265:195–201
Peltier WR (2004) Global glacial isostasy and the surface of the ice-age Earth: the ICE-5G (VM2) model and GRACE. Ann Rev Earth Planet Sci 32:111–149
Petit JR et al. (1999) Climate and atmospheric history of the past 420000 years from the Vostok Ice Core, Antarctica. Nature 399:429–436
Polyakov IV et al (2002) Observationally based assessment of polar amplification of global warming. Geophys Res Lett 29(18):1878
Poutou E (2003) Etude numérique du rôle des interactions entre la surface et l'atmosphère dans le cadre d'un changement climatique aux hautes latitudes nord, Grenoble, p 318
Raynaud D et al (1997) Air content along the GRIP core: a record of surface climatic parameters and elevation in Central Greeland. J Geophys Res 102:26607–26613
Renssen H et al (2005a) Simulating the Holocene climate evolution at northern high latitudes using a coupled atmosphere-sea ice-ocean-vegetation model. Clim Dyn 24:23–43
Renssen H et al (2005b) The Holocene climate evolution in the high latitude southern hemisphere simulated by a coupled atmosphere sea ice ocean vegetation model. Holocene (in press)

Rignot E, Thomas RH (2002) Mass balance of polar ice sheets. Science 297:1502–1506

Rind D et al (1997) The role of sea-ice in $2\times CO_2$ climate model sensitivity. 2. Hemispheric dependencies. Geophys Res Lett 24:1491–1494

Ritz C et al (2001) Modeling the evolution of Antarctic ice sheet over the last 420000 years: implications for altitude changes in the Vostok region. J Geophys Res 106(D23):31943–31964

Steig E et al (1998) Synchronous climate changes in Antarctica and the North Atlantic. Science 282:92–95

Stenni B et al (2003) A high resolution site and source late glacial temperature record derived from the EPICA Dome C isotope records (East Antarctica). EPSL 217:183–195

Stenni B et al (2001) An oceanic cold reversal during the last deglaciation. Science 293:2074–2077

Tarasov L, Peltier WR (2003) Greenland glacial history, borehole contraints and Eemian extent. J Geophys Res 108. DOI 10 1029/2001JB001731

Vaughan DG et al (2003) Recent rapid regional climate warming on the Antarctic Peninsula. Clim Change 60:243–274

Vavrus S, Harrison SP (2003) The impact of sea ice dynamics on the Arctic climate system. Clim Dyn 20:741–757

Watanabe et al (2003) A first comparison of the Dome Fuji and Vostok isotopic climate records. Memoirs of the National Institute for Polar Research, Tokyo, Japan

Werner M et al (2001) Isotopic composition and origin of polar precipitation in present and glacial climate simulations. Tellus 53B:53–71

Werner M, Tegen I, Harrison SP, Kohfeld KE, Colin IC, Balkanski Y, Rodhe H, Roelandt C (2002) Seasonal and interannual variability of the mineral dust cycle under present and glacial climate conditions. J Geophys Res 107. DOI10.1029/2002JD002365

Werner M et al (2000) Borehole versus isotope temperatures on Greenland: Seasonality does matter. Geophys Res Lett 27:723–726

Wohlfahrt J et al (2004) Synergetic feedbacks between ocean and vegetation on mid- and high- latitude climates during the mid-Holocene. Clim Dyn 22:223–238

Climate Dynamics (2006) 27: 437–440
DOI 10.1007/s00382-006-0149-1

PUBLISHER'S ERRATUM

V. Masson-Delmotte · M. Kageyama
P. Braconnot · S. Charbit · G. Krinner
C. Ritz · E. Guilyardi · J. Jouzel · A. Abe-Ouchi
M. Crucifix · R. M. Gladstone · C. D. Hewitt
A. Kitoh · A. N. LeGrande · O. Marti
U. Merkel · T. Motoi · R. Ohgaito · B. Otto-Bliesner
W. R. Peltier · I. Ross · P. J. Valdes
G. Vettoretti · S. L. Weber · F. Wolk · Y. Yu

Past and future polar amplification of climate change: climate model intercomparisons and ice-core constraints

Published online: 19 May 2006

1 Climate Dynamics (2006) 26: 513–529

Unfortunately, author corrections to Figs. 2, 3a, b, and 4a, b were not carried out.

The correct versions are shown below.

The online version of the original article can be found at http://dx.doi.org/10.1007/s00382-005-0081-9

V. Masson-Delmotte (✉) · M. Kageyama · P. Braconnot
S. Charbit · E. Guilyardi · J. Jouzel · O. Marti
Laboratoire des Sciences du Climat et de l'Environnement,
(LSCE/IPSL, UMR CEA-CNRS 1572) L'Orme des Merisiers,
Bâtiment 701, CEA Saclay, 91 191 Gif-sur-Yvette Cedex, France
E-mail: valerie.masson@cea.fr

G. Krinner · C. Ritz
Laboratoire de Glaciologie et de Géophysique de l'Environnement,
(UMR 5183 CNRS-UJF), Domaine Universitaire,
St Martin d'Hères, France

A. Abe-Ouchi
Center for Climate System Research,
The University of Tokyo, Kashiwa 277-8568, Japan

M. Crucifix · C. D. Hewitt
Hadley Centre for Climate Prediction and Research,
Met Office, FitzRoy Road, Exeter, EX1 3 PB Devon, UK

R. M. Gladstone · I. Ross · P. J. Valdes
School of Geographical Sciences,
University of Bristol, University Road,
Bristol BS8 1SS, UK

A. Kitoh · T. Motoi
Climate Research Department,
Meteorological Research Institute, 1-1 Nagamine, Tsukuba,
Ibaraki 305-0052, Japan

A. N. LeGrande
NASA Goddard Institute for Space Studies
and Center for Climate Systems Research,
Columbia University, New York, NY, USA

U. Merkel
IFM-GEOMAR, Duesternbrooker Weg 20,
24105 Kiel, Germany

R. Ohgaito · A. Abe-Ouchi
Frontier Research Center for Global Change (FRCGC),
JAMSTEC, Yokohama City 236-0001, Japan

B. Otto-Bliesner
Climate Change Research, National Center for Atmospheric
Research, 1850 Table Mesa Drive, P.O. Box 3000,
Boulder, CO 80307, USA

W. R. Peltier · G. Vettoretti
Department of Physics, University of Toronto,
60 St. George Street, Toronto
ON M5S 1A7, Canada

S. L. Weber
Climate Variability Research, Royal Netherlands
Meteorological Institute (KNMI),
P.O. Box 201, 3730 AE De Bilt,
The Netherlands

F. Wolk
Institut d'Astronomie et de Géophysique G. Lemaître,
Université catholique de Louvain, Chemin du cyclotron, 2,
1348 Louvain-la-Neuve, Belgium

Y. Yu
LASG, Institute of Atmospheric Physics,
Chinese Academy of Sciences,
P.O. Box 9804, Beijing 10029,
People's Republic of China

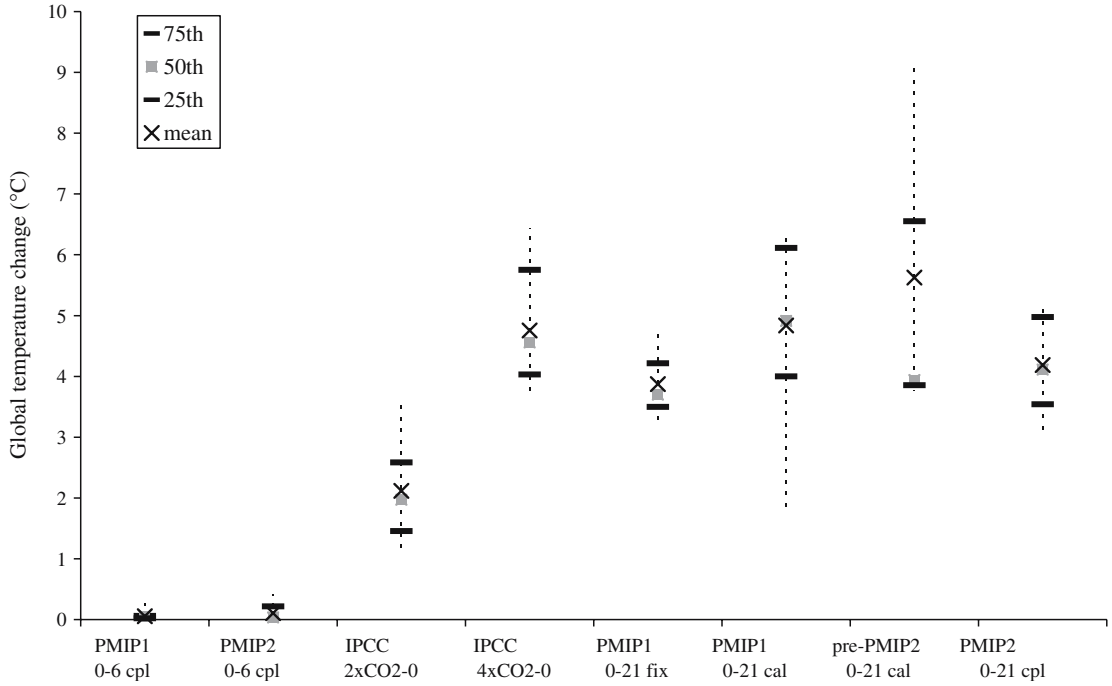

Fig. 2 Annual mean global temperature changes simulated by a variety of climate models run under similar boundary conditions. The full range (*dashed line*), mean (*cross symbol*), 25th (*lower bold dash symbol*), 50th (*grey square symbol*), 75th (*upper bold dash symbol*) percentiles of the various model results are calculated from the distribution of the various model results (see Table 2). The "fix", "slab" and "cpl" abbreviations refer to different configurations of models used and are described in Sect. 3 and Table 1

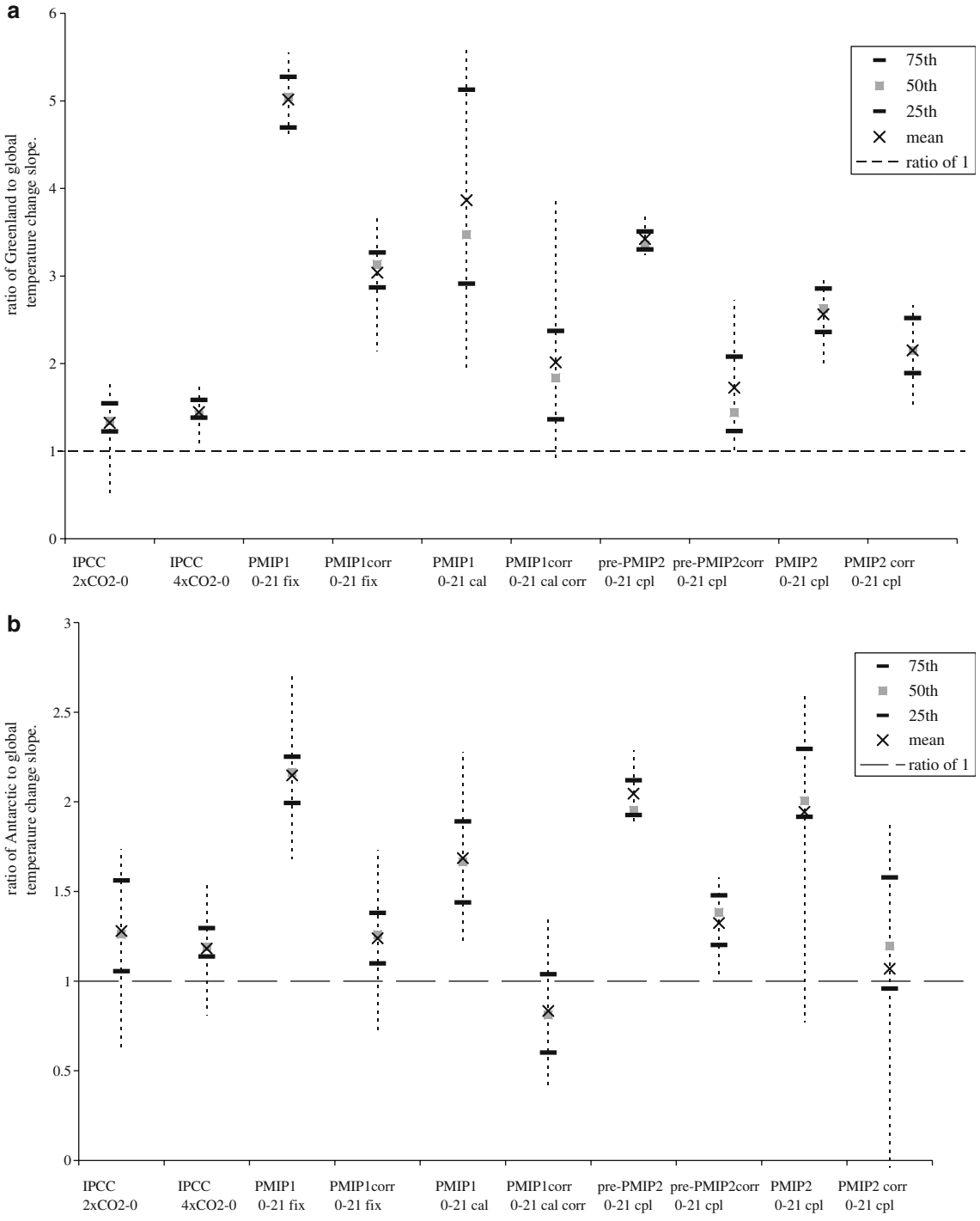

Fig. 3 a Central Greenland polar amplification (defined as the ratio between central Greenland and global annual mean temperature changes) simulated by climate models. The full range (*dashed line*), mean (*cross symbol*), 25th (*lower bold dash symbol*), 50th (*grey square symbol*), 75th (*upper bold dash symbol*) percentiles of the various model results are calculated from the distribution of the various model results (see Table 2). "corr" stands for elevation-corrected temperature values (see text). **b** Same as (**a**) but for central eastern Antarctica. Note that the vertical scale is half as small as for Greenland

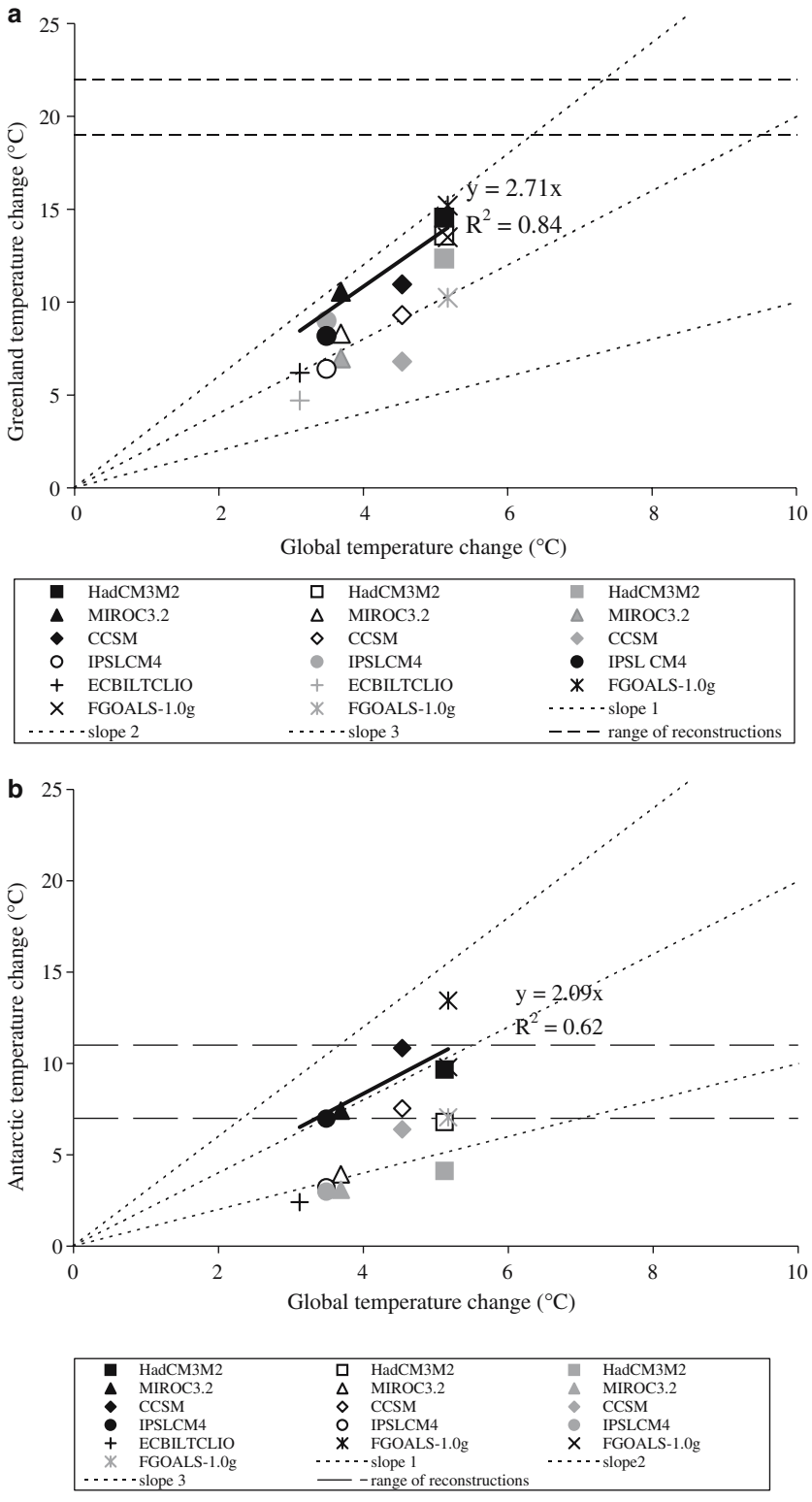

Fig. 4 **a** Comparison of Last Glacial Maximum to control central Greenland annual mean temperature change simulated by climate models (PMIP2 coupled ocean-atmosphere simulations only) with the range of paleoclimatic reconstructions. *Filled black squares* show direct model results. *Open black squares* show model results corrected from LGM to control ice sheet elevation changes (''elevation corrected'' results). *Grey squares* show model results corrected from elevation changes and precipitationweighted (''seasonality corrected'' results). *Horizontal long-dashed lines* reflect the range of temperature change derived from Greenland borehole thermometry. *Short dashed lines* correspond to slopes of 1, 2 and 3 for reference. A linear regression calculated on the results of these four models is also displayed (*solid black line* and regression result). Values below zero are not displayed (results of ECBILT CLIO with corrections. **b** Same as (**a**) but for central Antarctica. *Horizontal long-dashed lines* reflect the range of temperature change derived from Antarctic ice core water stable isotopes. **c** Same as (**a**) but for future climate change simulations. *Open black squares* represent 4 $\times$ CO_2 simulation anomalies, and *filled black rhomboids* 2 $\times$ CO_2 simulation anomalies. The *solid line* is a linear regression on all the simulation results. The *black dashed lines* represent lines with slopes of 1 and 2. **d** Same as (**b**) but for future climate change simulations. *Open black squares* represent 4 $\times$ CO_2 simulation anomalies, and *filled black rhomboids* 2 $\times$ CO_2 simulation anomalies. The *solid line* is a linear regression on all the simulation results. The *black dashed lines* represent lines with slopes of 1 and 2